Inorganic Chemistry
Communication

Inorg. Chem. **2010**, *49*, 2017–2019 **2017**
DOI: 10.1021/ic902107u

Niobium-Complex-Based Syntheses of Sodium Niobate Nanowires Possessing Superior Photocatalytic Properties

Kenji Saito*,†,‡ and Akihiko Kudo*,†

†*Department of Applied Chemistry, Faculty of Science, Tokyo University of Science, 1-3 Kagurazaka, Shinjyuku-Ku, Tokyo 162-8601, Japan, and* ‡*PRESTO, Japan Science and Technology Agency (JST), 4-1-8 Honcho, Kawaguchi, Saitama 332-0012, Japan*

Received October 24, 2009

Sodium niobates with nanowire morphology ($NaNbO_3$-NW) were synthesized in a large scale by use of a niobium oxooxalate complex as the starting material. This $NaNbO_3$-NW showed definitely enhanced photocatalytic activity for H_2 or O_2 evolution in the presence of sacrificial reagents and an overall water splitting under UV-light irradiation, as compared with a bulky counterpart ($NaNbO_3$-B). This is the first example that an overall water splitting into H_2 and O_2 proceeded on the semiconductor nanowire photocatalyst.

Water splitting using powder photocatalysts has attracted much attention because of one of the substantial resolutions with respect to recent rapid consumption of the fossil fuels, in addition to the rising concern of the environmental issues caused by the use of fossil fuels.[1,2a] A conventional solid-state reaction for the preparation of photocatalysts for water splitting or the half-reaction of H_2 or O_2 evolution in the presence of a sacrificial reagent generally gives relatively large particles. The particle size typically affects the photocatalytic properties. Therefore, the preparation of particles with small and uniform size is one key issue. For example, a small particle size diminishes the distance of transfer of the photogenerated carrier from the bulk to the surface.[2b] Another critical point among factors affecting the photocatalytic properties is structural anisotropy because of promotion of the charge separation associated with inhibition of the charge recombination process.[2c] In this context, a nanowire-shaped semiconductor photocatalyst has merited special attention.[3] So far, efforts devoted to the development of semiconductor nanowires possessing superior photocatalytic properties have often been hampered.[4] This would arise from less crystallinity and the existence of grain boundaries in the resulting nanowires. Recently, we have reported that a niobium oxooxalate complex was able to be employed as the starting material for the synthesis of the TT phase of niobium pentoxide nanowires with high crystallinity and relatively large surface areas. This nanowire exhibited higher photocatalytic properties than bulky niobia.[5] This result has prompted us to design the complex oxide photocatalyst. We have selected a $NaNbO_3$ photocatalyst for the preparation of nanowires because it is the niobate showing activities for water splitting and H_2 or O_2 evolution in the presence of sacrificial reagents.[6,7] In the present study, the large-scale preparation of nanowires of $NaNbO_3$ photocatalysts was investigated using a niobium oxooxalate complex as the starting material.

All solvents and chemicals were of reagent-grade qualities and were used without further purification. The typical procedures to synthesize $NaNbO_3$-NW and $NaNbO_3$-B were as follows. A mixture of the niobium complex, $(NH_4)_3[NbO(ox)_3]\cdot H_2O$ (2 g, 4.5 mmol),[8] and an equimolar amount of NaOH was heated in trioctylamine (TOA; 50 mL) of a structure-directing solvent at 573 K for 2.5 h. The resulting suspension was filtered, and the solids were calcined in air at 773 K for 5 h, followed by washing with water to obtain $NaNbO_3$-NW (0.6 g, 3.7 mmol). $NaNbO_3$-B was prepared by a conventional solid-state method. Nb_2O_5 (Kanto Chemical; 99.95%) and Na_2CO_3 (Kanto Chemical; 99.8%) were used as starting materials, and the mixtures were calcined in air at 1173 K for 6 h. The powders obtained were characterized by powder X-ray diffraction (XRD; Rigaku Miniflex, Cu Kα). Scanning electron microscopy (SEM) images were taken

*To whom correspondence should be addressed. E-mail: ksaito@rs.kagu.tus.ac.jp (K.S.), (A.K.).

(1) Fujishima, A.; Honda, K. *Nature* **1972**, *37*, 238.
(2) (a) Kudo, A.; Miseki, Y. *Chem. Soc. Rev.* **2009**, *38*, 253. (b) Miseki, Y.; Saito, K.; Kudo, A. *Chem. Lett.* **2009**, *38*, 180. (c) Miseki, Y.; Kato, H.; Kudo, A. *Energy Environ. Sci.* **2009**, *2*, 306.
(3) (a) Xu, C.-Y.; Zhen, L.; Yang, R.; Wang, Z. L. *J. Am. Chem. Soc.* **2007**, *129*, 15444. (b) Ke, T.-Y.; Chen, H.-A.; Sheu, H.-S.; Yeh, J.-W.; Lin, H.-N.; Lee, C.-Y.; Chiu, H.-T. *J. Phys. Chem. C* **2008**, *112*, 8827. (c) Li, L.; Deng, J.; Chen, J.; Sun, X.; Yu, R.; Liu, G.; Xing, X. *Chem. Mater.* **2009**, *21*, 1207.
(4) (a) Bao, N.; Shen, L.; Takata, T.; Lu, D.; Domen, K. *Chem. Lett.* **2006**, *35*, 318. (b) Yu, J.; Kudo, A. *Adv. Funct. Mater.* **2006**, *16*, 2163. (c) Jitputti, J.; Pavasupree, S.; Suzuki, Y.; Yoshikawa, S. *Jpn. J. Appl. Phys.* **2008**, *47*, 751. (d) Ding, Q.-P.; Yuan, Y.-P.; Xiong, X.; Li, R.-P.; Huang, H.-B.; Li, Z.-S.; Yu, T.; Zou, Z.-G.; Yang, S.-G. *J. Phys. Chem. B* **2008**, *112*, 18846. (e) Song, S.; Zhang, Y.; Xing, Y.; Wang, C.; Feng, J.; Shi, W.; Zheng, G.; Zhang, H. *Adv. Funct. Mater.* **2008**, *18*, 2328.
(5) Saito, K.; Kudo, A. *Bull. Chem. Soc. Jpn.* **2009**, *82*, 1030.
(6) Li, G.; Kako, T.; Wang, D.; Zou, Z.; Ye, J. *J. Phys. Chem. Solids* **2008**, *69*, 2487.
(7) Iwase, A.; Saito, K.; Kudo, A. *Bull. Chem. Soc. Jpn.* **2009**, *82*, 514.
(8) Bayot, D. A.; Devillers, M. M. *Inorg. Chem.* **2006**, *45*, 4407.

Published on Web 01/26/2010

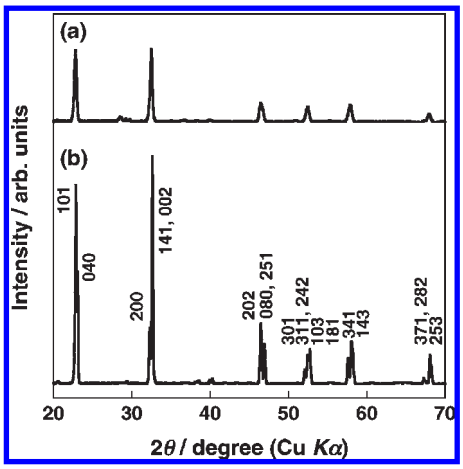

Figure 1. XRD patterns of (a) $NaNbO_3$-NW and (b) $NaNbO_3$-B.

using a JEOL JSM-6700F microscope. Transmission electron microscopy (TEM) images were collected with a Hitachi H-9500 microscope operating at an accelerating voltage of 200 kV. Brunauer−Emmett−Teller surface areas were measured with a Coulter SA 3100 apparatus using nitrogen as the adsorbing gas. Diffuse-reflection spectra were recorded on a UV−vis−near-IR spectrometer (Jasco; UbestV-570) and were converted from reflection to absorbance by the Kubelka−Munk method. Photocatalytic water splitting was carried out in an inner irradiation reaction cell made of quartz to irradiate intensive UV light using a 400 W high-pressure mercury lamp (SEN HL400EH-5). A reaction cell with a top window made of Pyrex and a 300 W xenon-arc lamp (Perkin-Elmer Cermax-PE300BF) was used for H_2 evolution from an aqueous methanol solution and O_2 evolution from an aqueous silver nitrate solution to prevent not photocatalytic but photochemical H_2 evolution from an aqueous methanol solution by intensive UV light from a 400 W high-pressure mercury lamp with an inner irradiation cell made of quartz. These reaction cells were connected to a gas-closed circulation system with an online gas chromatograph.[2] Platinum cocatalysts for H_2 evolution were loaded on photocatalysts using a conventional photodeposition method from H_2PtCl_6 as the metal source in situ. A RuO_2 cocatalyst for an overall water splitting was deposited on a photocatalyst by an impregnation method from an acetone solution containing $Ru_3(CO)_{12}$,[9] and the impregnated powder was calcined at 673 K for 1 h in air. Apparent quantum yields (AQYs) were measured using a 300 W xenon illuminator (Asahi Spectra MAX-301) with a band-pass filter (Asahi Spectra) as the light source. The AQY was determined according to eq 1:

$$\begin{aligned} \text{AQY}\ (\%) &= \frac{\text{no. of reacted electrons}}{\text{no. of incident photons}} \times 100 \\ &= \frac{\text{no. of evolved } H_2 \text{ molecules} \times 2}{\text{no. of incident photons}} \times 100 \end{aligned} \quad (1)$$

Crystal structures of the powders obtained were characterized by XRD as shown in Figure 1. The diffraction peaks of $NaNbO_3$-NW were indexed with the orthorhombic $NaNbO_3$ phase (PDF 33-1270), in conjunction with minor species.

(9) Inoue, Y. *Energy Environ. Sci.* **2009**, *2*, 364.

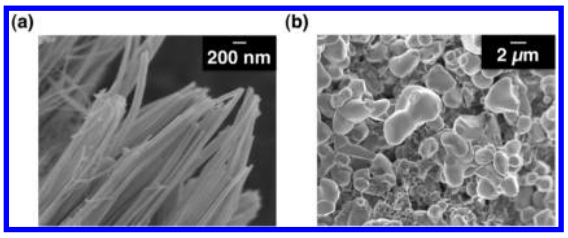

Figure 2. SEM patterns of (a) $NaNbO_3$-NW and (b) $NaNbO_3$-B.

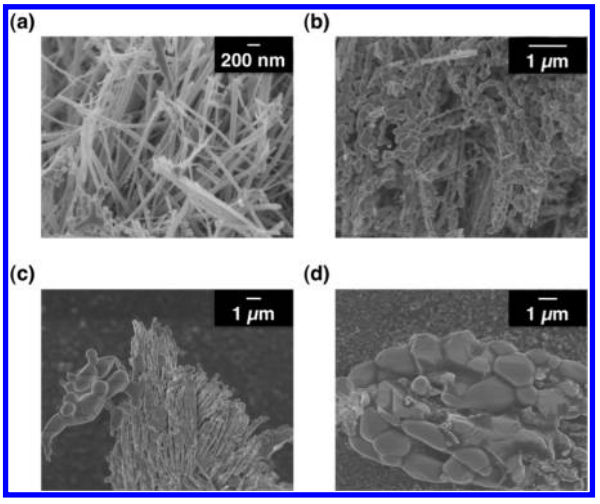

Figure 3. SEM images of $NaNbO_3$-NW calcined at 973 K for 5 h (a and b) and at 1273 K for 5 h (c and d).

$NaNbO_3$-NW possessed less crystallinity than $NaNbO_3$-B, judging from the half-widths of the peaks.

The SEM image of $NaNbO_3$-NW indicated the nanowire morphology with relatively uniform size (lengths of up to several micrometers) being different from that of $NaNbO_3$-B showing characterless large particles, as shown in Figure 2.[5] Such characterless particles were hardly observed for $NaNbO_3$-NW. Convergent-beam electron diffraction indicated that $NaNbO_3$-NW possesses a single-crystalline nature, and the direction of the nanowires is determined to be [010] (Figure S1a in the Supporting Information). The high-resolution TEM (HR-TEM) image shown in Figure S1b in the Supporting Information indicated a lattice fringe, and the width of the fringe was 2.82 ± 0.07 Å, corresponding to a (200), (141), or (002) crystal plane, not stemming from niobia. The nanowire growth could be explained by the following machanism. TOA coordinates to the niobium complex associated with dissociation of the oxalate ligand under heat treatment, in addition to the occurrence of a partial or complete exchange reaction of an ammonium countercation to a sodium ion, below the decomposition temperature of oxalic acid, followed by self-assembly to each other via hydrophobic interaction between the octyl chains in TOA. Then, such an assembly undergoes directional growth for forming nanowire structures to form $NaNbO_3$-NW. The thermal stability of the nanowire structure was also examined by changing the calcination temperature. $NaNbO_3$-NW calcined at 973 K showed apparently a half-and-half mixture of the nanowire structures (Figure 3a) and small particles (Figure 3b). Calcination at 1273 K mainly afforded large particles (Figure 3d), in conjunction with partially maintained nanowire structures as minor species (Figure 3c).

Table 1. Photocatalytic H_2 or O_2 Evolution from 10 vol % of an Aqueous Methanol Solution or a 0.02 M Aqueous Silver Nitrate Solution over $NaNbO_3$-NW and $NaNbO_3$-B[a]

			rate of gas evolution/μmol h^{-1}	
photocatalyst	cocatalyst	surface area/m^2 g^{-1}	H_2	O_2
$NaNbO_3$-NW	none	38	1.3	13
$NaNbO_3$-NW	Pt (0.1 wt %)	38	44	
$NaNbO_3$-NW	Pt (0.3 wt %)	38	74	
$NaNbO_3$-NW	Pt (0.5 wt %)	38	130	
$NaNbO_3$-NW	Pt (0.7 wt %)	38	120	
$NaNbO_3$-NW	Pt (1.0 wt %)	38	110	
$NaNbO_3$-B	none	0.4	2.7	9.7
$NaNbO_3$-B	Pt (0.1 wt %)	0.4	40	
$NaNbO_3$-B	Pt (0.3 wt %)	0.4	32	
$NaNbO_3$-B	Pt (0.5 wt %)	0.4	19	
$NaNbO_3$-B	Pt (1.0 wt %)	0.4	19	

[a] Reaction conditions: catalyst, 0.1 g; reactant solution, 150 mL; light source, 300 W xenon-arc lamp ($\lambda > 300$ nm); cell, top-irradiation cell with a Pyrex glass window.

Although the diffuse-reflection spectrum of $NaNbO_3$-NW was different from that of $NaNbO_3$-B in their absorption features, these spectra possessed almost the same absorption edge at 3.4 eV, indicating no influence on the band gap by shape transformation (Figure S2 in the Supporting Information).

H_2 and O_2 evolution reactions were carried out in the presence of sacrificial reagents under UV-light irradiation, as summarized in Table 1. Photocatalytic H_2 evolution proceeded on both $NaNbO_3$-NW and $NaNbO_3$-B powders. The absence of a cocatayst afforded negligible activities, i.e., 2.7 and 1.3 μmol h^{-1}, respectively, and, thus, both of them seem to be similar to each other. In contrast, $NaNbO_3$-NW showed enhanced photocatalytic activities compared with $NaNbO_3$-B when a platinum cocatalyst was loaded on the photocatalysts. Here, the difference in the optimized amounts of platinum cocatalyst mainly arises from the surface area. In general, a large surface area affords a high dispersion of cocatalyst particles that contribute to the enhancement of the photocatalytic property. To check the influence of the wavelength on H_2 evolution, we have measured the action spectra of both samples loaded with optimized amounts of platinum (Figure S3 in the Supporting Information). At >300 nm, $NaNbO_3$-NW showed higher AQYs than $NaNbO_3$-B even if the absorbance of $NaNbO_3$-NW was smaller than that of $NaNbO_3$-B. The photocatalytic activity of $NaNbO_3$-NW for water photooxidation to form O_2 was also enhanced. We have also examined the overall water splitting by employing a RuO_2 cocatalyst. $NaNbO_3$-NW showed the photocatalytic activity for the water-splitting reaction as shown in Figure 4, in contrast to $NaNbO_3$-B. This is the first example of an overall water splitting over a nanowire-shaped semiconductor photocatalyst. The intrinsic stability of $NaNbO_3$-NW in the course of the photocatalytic experiment was confirmed with XRD by use of the sample after long-time photoillumination (Figure S4 in the Supporting Information). The XRD patterns obtained were the same as those before photoillumination.

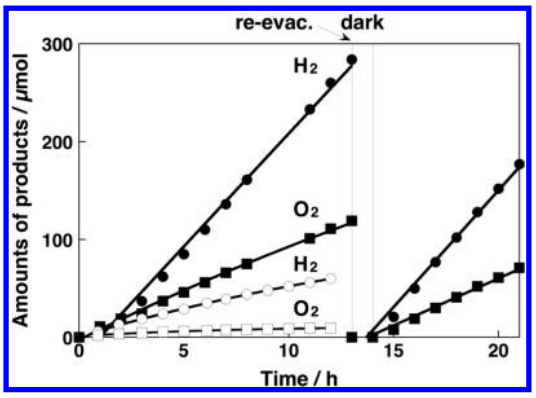

Figure 4. Overall water splitting over (a) RuO_2 (5 wt %)/$NaNbO_3$-NW (black circles and squares) and (b) RuO_2 (5 wt %)/$NaNbO_3$-B (white circles and squares). Reaction conditions: catalyst, 0.3 g; pure water, 350 mL; inner irradiation cell made of quartz; 400 W high-pressure mercury lamp.

The reason why $NaNbO_3$-NW possesses superior photocatalytic properties compared with $NaNbO_3$-B mainly originates from small particle sizes, the structural anisotropy seen in Figure 2a, and large surface areas as shown in Table 1. Inhibition of the grain boundary, crystallinity, and exposure of the crystal plane active for photocatalytic reaction would also contribute to this matter. Thus, the development of semiconductor nanowires possessing these superior factors will be important for effcient light-energy conversion systems.

In conclusion, we have successfully developed a complex oxide nanowire possessing superior photocatalytic properties in a large scale by the proper combination of a niobium complex and a structure-directing agent. Although the semiconductor nanowire can be synthesized by a dry process as represented by a chemical vapor deposition technique,[10] devising a strategy for nanowire synthesis based on a wet process offers the opportunity for gram-scale synthesis of such a nanowire,[3] enabling us to apply it to a functional material such as a photocatalyst. This method opens a new strategy toward development of a variety of niobium-based complex oxide semiconductor nanowires and efficient water-splitting systems.

Acknowledgment. This work was supported by the JST PRESTO (Precursory Research for Embryonic Science and Technology) program, a Grant-in-Aid for Young Scientists B (Grant 20750113) from the Ministry of Education, Culture, Sports, Science and Technology (MEXT) of Japan, the Sumitomo Foundation, the Mitsubishi Chemical Corp. Fund, and the Nissan Science Foundation.

Supporting Information Available: Convergent-beam electron diffraction (Figure S1a) and a HR-TEM image (Figure S1b) of $NaNbO_3$-NW, diffuse-reflection spectra of $NaNbO_3$-NW and $NaNbO_3$-B (Figure S2), action spectra for H_2 evolution from 10 vol % aqueous methanol solutions over Pt (0.5 wt %)/$NaNbO_3$-NW and Pt (0.1 wt %)/$NaNbO_3$-B (Figure S3), and XRD patterns of RuO_2 (5 wt %)/$NaNbO_3$-NW before and after photoillumination (Figure S4). This material is available free of charge via the Internet at http://pubs.acs.org.

(10) Bae, C.; Yoo, H.; Kim, S.; Lee, K.; Kim, J.; Sung, M. M.; Shin, H. *Chem. Mater.* **2008**, *20*, 756.